Effect of Polycarbonate Molecular Weight on Polymer Blends of Polycarbonate and ABS

JIANN-SHING WU,* SHU-CHEN SHEN, and FENG-CHIH CHANG

Institute of Applied Chemistry, National Chiao Tung University, Hsinchu, Taiwan, Republic of China

SYNOPSIS

The melt viscosity of polycarbonate/acrylonitrile-butadiene-styrene (PC/ABS) blends relative to PC is significantly lower, even lower than that of pure ABS in some compositions. Annealing above the T_g of PC coalesces and coarsens phase structure in core and skin regions. Increase in the molecular weight of PC in PC/ABS blends results in low-temperature fracture toughness improvement but suffers from the disadvantage of higher melt viscosity. The selection of PC in PC/ABS blends must be a compromise between the toughness advantages of higher PC molecular weight and the disadvantages of higher melt viscosity. © 1993 John Wiley & Sons, Inc.

INTRODUCTION

Polymer science and technology have undergone tremendous growth during the last two decades, particularly through chemical diversification. The concept of physically blending two or more existing polymers to create new products has attracted great interest and resulted in wide commercial utilization. Polymer blends of polycarbonate (PC) with acrylonitrile-butadiene-styrene (ABS) provide a balance of toughness, heat resistance, and ease of processing at a cost lower than that of the high-performance thermoplastic PC. Since the appearance of the first PC/ABS patent nearly three decades ago,[1] blends or alloys of PC/ABS have been some of the most successful commercial polyblend products. Numerous key patents have been issued[2-9] specifically dealing with many aspects of properties, such as heat distortion temperature, impact strength, processability, or flame resistance. Fundamental studies of PC/ABS blends in terms of mechanical, rheological, morphological, and thermodynamic properties have been extensively reported in the open literature.[10-26] However, only limited work has been reported concerning, specifically, the effect of PC molecular weight in PC-ABS blends. Most literature do not give reasons why the particular PC or ABS was selected in their studies. Molecular weight of the blend component is an important variable, especially as a major component, that can significantly influence essentially all the above-mentioned properties of the resultant PC/ABS blends. The main objective of this study is to obtain a better understanding of the effect of changing the PC molecular weight and to provide better guidance for proper selection of the starting materials in the PC/ABS blends.

EXPERIMENTAL

Materials

Natural grades of PCs, Calibre®, from Dow Chemical Co. with melt flow rates (MFR) of 3, 6, 10, 15, 20, and 60 were used in this study (Table I). PC with MFR = 15 (PC15) was considered as the general purpose grade and was selected as the blend component in this PC/ABS polyblend studies when the PC molecular weight was not treated as a variable. ABS with 18% rubber content was obtained from Grand Pacific Petrochemical Corp. of Taiwan.

Melt Blending and Specimens Preparation

Melt blending was prepared by a corotating 30 mm-diameter twin-screw extruder with an L/D ratio of 29. The standard ASTM $\frac{1}{8}$ in. specimens were pre-

* To whom correspondence should be addressed.

Journal of Applied Polymer Science, Vol. 50, 1379-1389 (1993)
 CCC 0021-8995/93/081379-11

Table I Melt Flow Rate and Molecular Weight of PCs

MFR	M_w	M_n
3	35,900	13,300
6	31,500	11,600
10	28,200	10,600
15	25,100	9,700
20	24,100	9,600
60	18,100	8,300

Data extracted from Refs. 29 and 30.

pared using an Arburg 3 oz injection-molding machine. The temperatures of extrusion and injection molding were adjusted to give the optimized processing conditions according to the blending compositions and the materials selected. Component weight ratio, PC/ABS = 65/35, was close to most commercially available products and was chosen to study the effect of PC MFR in this study.

Characterizations

The melt rheological properties were examined by a capillary rheometer, Model Rheograph 2001, Gottfert, Germany. Procedures for the mechanical properties—tensile, flexural, and standard notched Izod impact at various temperatures—and the critical strain energy release rate (Gc) were described in our previous reports.[27-30] The injection-molded specimens were annealed as a function of time at 175°C under atmosphere conditions. Phase morphologies of the blends have been characterized by both transmission (TEM) and scanning electron microscopy (SEM). The fracture surfaces of the specimens were examined by SEM after etching with 30% KOH aqueous solution up to a maximum of 30 min, rinsing with water, and coating with gold. The TEM thin-layer specimens were cut by a microtome and stained with 2% OsO_4 solution for 6 h. The differential scanning calorimetry (DSC) measurements were carried out using a Seiko differential scanning calorimeter, Model SSC-5000. T_g was taken as the temperature at which the heat capacity reached one-half of the entire step change as observed on the thermogram.

RESULTS AND DISCUSSION

Melt Rheological Properties

The rheological properties of polyblend provide important information necessary to optimize process-

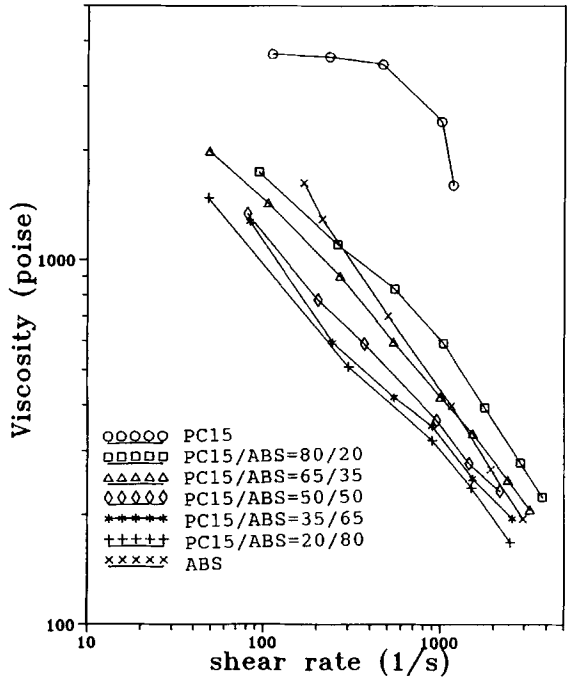

Figure 1 Melt viscosity vs. shear rate of PC15/ABS blends at 250°C.

ing conditions such as melt extrusion or injection molding. Figures 1 and 2 show the apparent melt viscosity vs. shear rate of PC15/ABS blends at 250°C. The presence of ABS, even at as low as 20%, is able to reduce the melt viscosity of PC significantly. The presence of 35% or higher ABS in the blends results in viscosity close to or even lower than ABS. A similar phenomenon was also reported previously.[21] The viscosity of polymeric materials changes greatly with temperature and the plots of $1/T$ vs. viscosity at constant shear rate (100 and

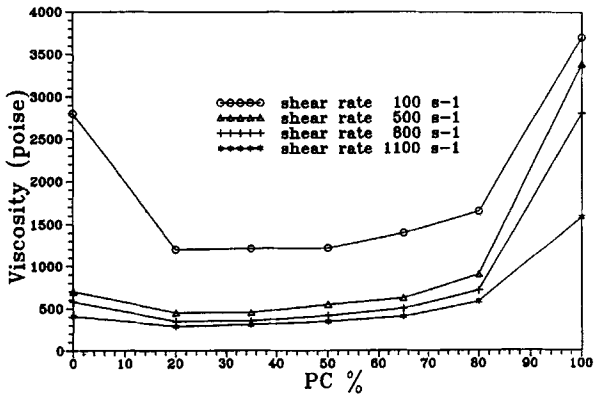

Figure 2 Melt viscosity vs. PC content of PC15/ABS blends at 250°C.

1000 s^{-1}) for PC15 and ABS are shown in Figures 3 and 4. The viscosities of PC15 and ABS are fairly close, 3700 vs. 2800 poise, at 250°C and low shear rate (100 s^{-1}, Fig. 3). At a higher shear rate of 1000 s^{-1}, the ABS viscosity is significantly lower than that of PC15, 470 vs. 2400 poise, as shown in Figure 4. That means that the viscosity of ABS in the typical PC/ABS blend processing temperatures is much more shear-sensitive than is that for PC. Figure 5 shows the effect of PC molecular weight on melt viscosity for the blends of PC15/ABS = 65/35 composition. PC with greater viscosity, due to higher PC molecular weight, also results in higher viscosity of the PC15/ABS blends, as would be expected.

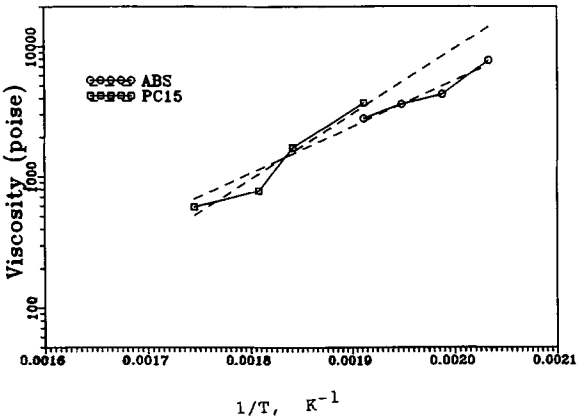

Figure 4 Plots of melt viscosity vs. $1/T$ for PC15 and ABS at higher shear rate of 1000 s^{-1}.

SEM and TEM Morphologies of the Blends

As mixtures of two polymers are deformed during flow, complex morphologies can develop. Pieces of one polymer may be drawn into filaments that may remain as filaments or break up into small drops or connect to each other to give an interconnected network. Under some conditions, ribbons or sheets of one polymer can be formed inside of the other polymer. Thus, rheologically related morphologies of polymer blends are very complex. By careful control of the etching condition, the features of phase domains can be obtained.

Figure 6 shows the SEM morphologies of the cryogenic fractured surfaces perpendicular to flow direction of the PC15/ABS blends with various component ratios. Figure 6(A) shows the SEM morphology of the blend containing 80% PC15. Since PC15 is the major and continuous phase in the blend, the fine particles shown in Figure 6(A) probably come from the ABS particles that have been etched out and recoated on the surface and this is certainly not the original morphology of the blend. The blends with 65 and 50% PC15 exhibit co-continuous morphologies as shown in Figure 6(B) and (C). Because of the higher viscosity of PC15 than that of ABS as mentioned earlier, the blend with 35% PC15 results in PC15 as a spherical and dispersed phase, as shown in Figure 6(D). Figure 6(E) shows the morphology of the blend with 20% PC15 where the volume fraction of these

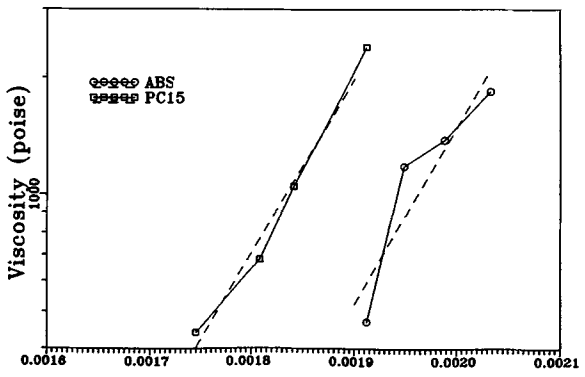

Figure 3 Plots of melt viscosity vs. $1/T$ for PC15 and ABS at lower shear rate of 100 s^{-1}.

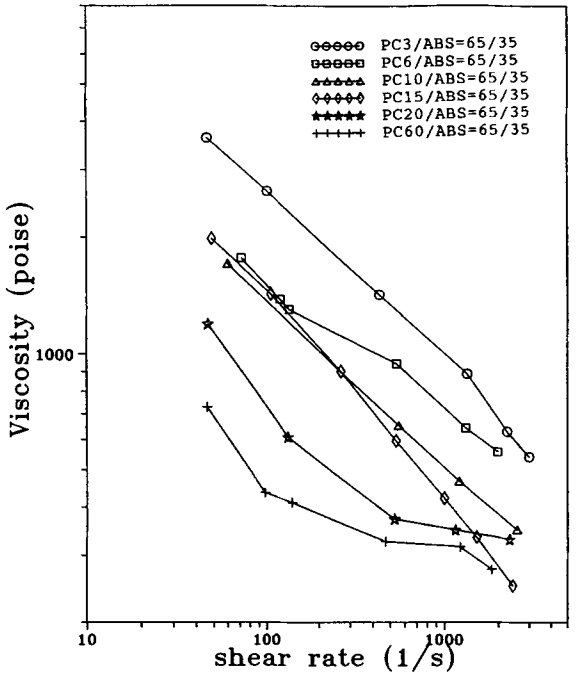

Figure 5 Melt viscosity vs. shear rate of PC/ABS = 65/35 blends by varying PC MFR.

A. PC15/ABS=80/20

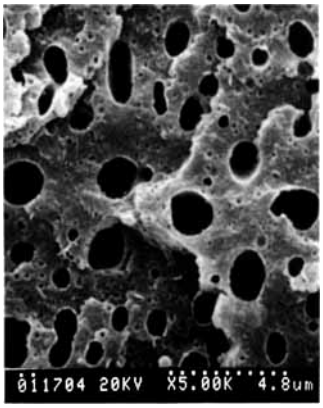

B. PC15/ABS=65/35

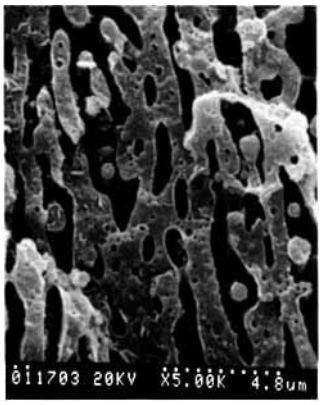

C. PC15/ABS=50/50

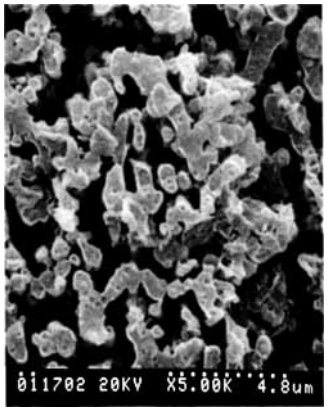

D. PC15/ABS=35/65

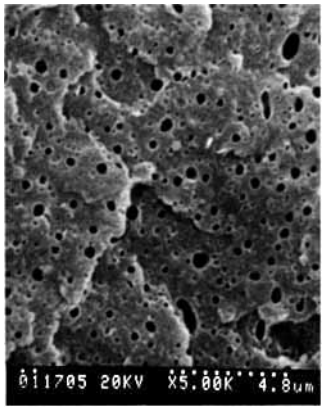

E. PC15/ABS=20/80

Figure 6 Etched SEM micrographs of PC15/ABS blends by varying component ratio: (A) PC15/ABS = 80/20; (B) PC15/ABS = 65/35; (C) PC15/ABS = 50/50; (D) PC15/ABS = 35/65; (E) PC15/ABS = 20/80.

spherical PC particle holes is estimated as less than 10%. This is an indication that a significant amount PC15 is dissolved in the ABS phase.

Figure 7 shows a few selected SEM morphologies of PC/ABS = 65/35 blends, by varying the MFR of PC, that were fractured in liquid nitrogen and under ambient conditions. The morphologies of the cryogenic fracture surfaces do not show significant differences [Fig. 7(A), (C), and 7(E)] among these blends. However, the more ductile blend (lower PC MFR) shows a much finer texture of the ambient fracture surface [compare Fig. 7(B), (D) and (F)]. Greater surface shear yielding of the more ductile blend reflects in the resultant finer texture of the etched surface morphology. Besides the above-mentioned complex factors dictating the phase morphology, the presence of rubber in this triple-phase blend was reported previously to promote compatibility between PC and SAN.[22] Figure 8 shows the TEM micrograph of the PC15/ABS = 50/50 blend where the rubber particles distributed in the SAN phase are irregular. This ABS is the blended product from a higher rubber content ABS and SAN, and this high-rubber ABS is the product directly from the polymerization reactor.

Effect of Annealing

Figure 9 shows the skin layer SEM micrographs of the PC15/ABS = 65/35 blend after annealing for different times. The skin layer possesses an oriented sheetlike, multilayer composite structure before annealing because of high shear during injection mold-

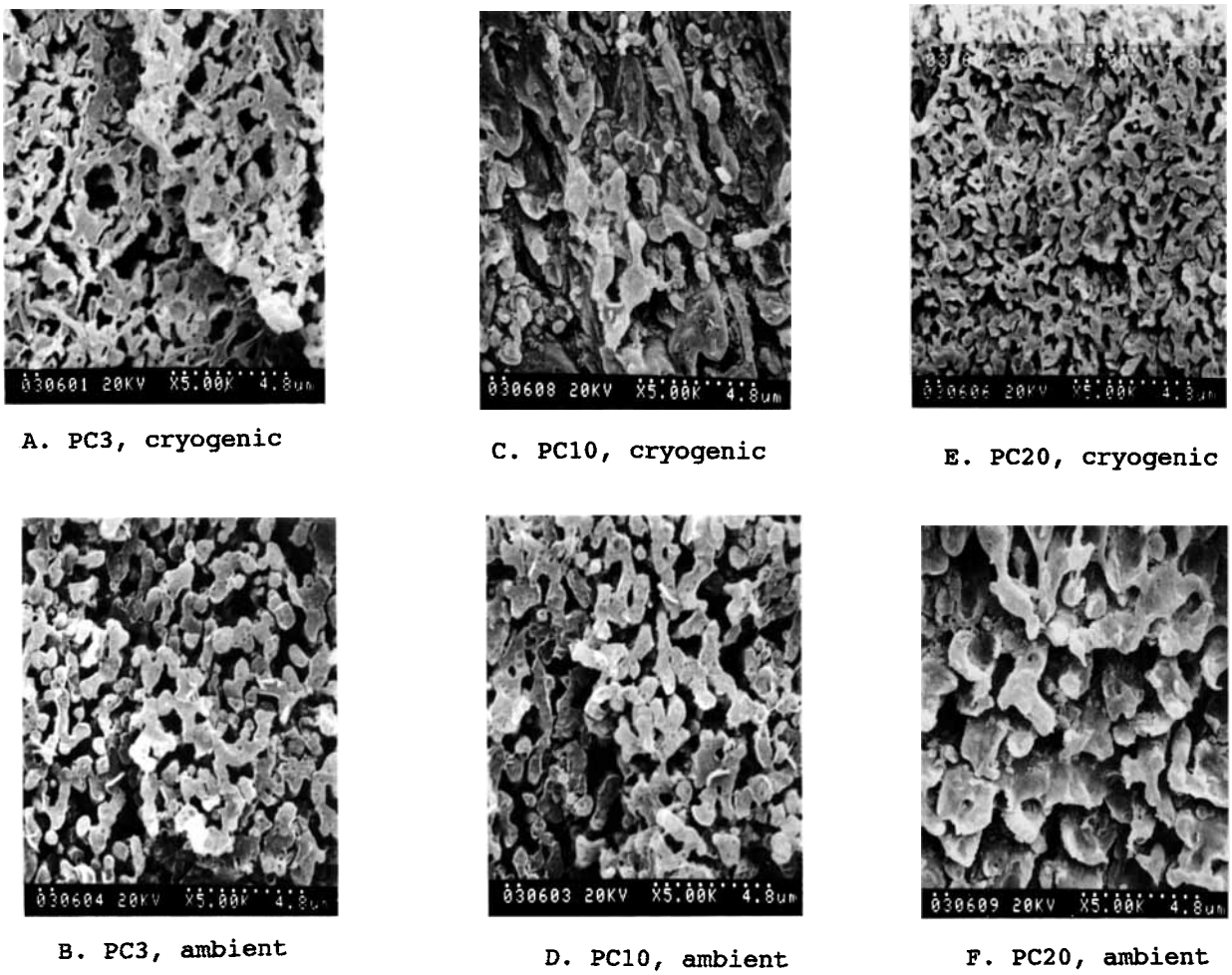

Figure 7 Etched SEM micrographs of the cryogenic and ambient fracture surfaces of PC/ABS = 65/35 blends by varying PC MFR: (A) PC3, cryogenic; (B) PC3, ambient; (C) PC10, cryogenic; (D) PC10, ambient; (E) PC20, cryogenic; (F) PC20, ambient.

ing [Fig. 9(A)]. After annealing, the multilayer-like skin structure appears to have restructured and creates large holes, as shown in Figure 9(B)–(D). Figure 10 shows the annealing effect on the core region taken from the fracture surfaces perpendicular to the direction of injection molding. Upon annealing, the phases coarsen and transform into a nearly dispersed type structure. Since the annealing temperature is significantly lower than the typical injection-molding temperature (175°C vs. 250°C), we would expect a much higher rate of phase coarsening at the melt-processing condition. Phase morphology coarsening of the PC/SAN system was previously reported.[24] When annealing above the T_g of PC under zero-shear condition, interfacial tension provides the driving force to coarsen the phases in this partially miscible PC/ABS blending system. The mechanisms contributing to the reduction in interfacial contact for this co-continuous system are considered to include coalescence, retraction, and thread breakup processes, in contrast to an occluded system that would require only coalescence of discrete particles.[24]

T_g of the Blends by DSC

Table II shows the T_g of the PC15/ABS with various compositions. The partial miscibility between PC and SAN has been well recognized. The T_g of the PC-rich phase decreases with the increase of ABS content, whereas the T_g of the SAN-rich phase increases with increase of PC content, as would be expected. The difference between ΔT_g(PC) in the PC-rich phase and ΔT_g(ABS) in the ABS-rich phase is insignificant. The observed ΔT_g(PC) and

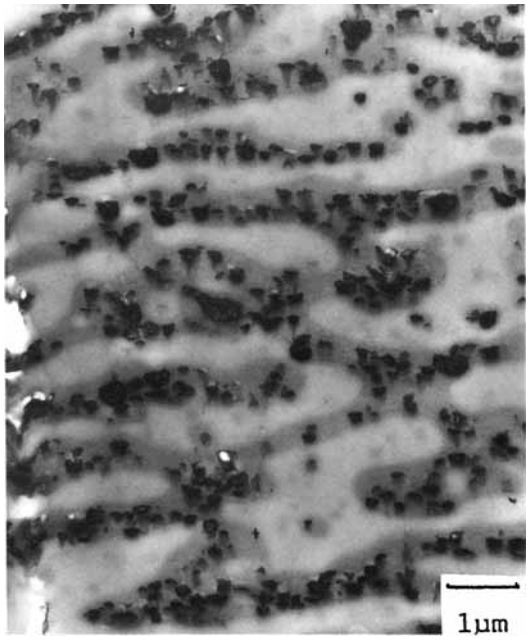

Figure 8 TEM micrograph of PC15/ABS = 65/35 blend.

ΔT_g(ABS) in the PC15/ABS = 50/50 blend are 11.4 and 9.5°C, respectively. Therefore, we expect the weight fraction of ABS dissolved in the PC-rich phase and the weight fraction of PC component dissolved in the ABS-rich phase to be comparable. Keitz et al.[16] also reported comparable ΔT_g(PC) and ΔT_g(SAN), 7.0°C vs. 6.6°C, in the PC/SAN = 50/50 blend with 26.7% AN content in SAN. Kim and Burns[22] reported greater ΔT_g(PC) (8.2°C) in the PC-rich phase than ΔT_g(ABS) (2.6°C) in the ABS-rich phase from the blend of PC/ABS = 50/50 and concluded that more of the ABS dissolved in the PC-rich phase than did the PC dissolve in the ABS-rich phase. Besides, the overall T_g shifts observed from our study are greater than those reported by Kim and Burns.[22]

The miscibility between PC and ABS depends on the acrylonitrile (AN) content in the SAN phase[16] and the 38.3% AN content in SAN employed by Kim and Burns appears to be higher than the optimized range for best miscibility for the PC/SAN blending system. Paul et al.[15] reported that 27% AN in SAN has the maximum adhesion between PC and SAN in their lap-shear tests. There is somewhat of a controversy on how much AN content provides the best compatibility between PC and SAN. However, AN content of 38.3% is believed to be higher than the optimized value for best compatibility. The AN content in SAN in the ABS that we employed is approximately 28%. The difference in AN content in SAN can explain the observed miscibility difference between our results and results from Kim and Burns.[22]

Table III shows the T_g of PC/ABS blends by varying PC MFR. The T_g shift of either the PC-rich or SAN-rich phase depends on mutual solubility. Higher PC molecular weight in the blend shows higher T_g and greater ΔT_g(PC) in the PC-rich phase, probably due to better mixing, and, therefore, more of the SAN dissolved in the PC phase. The ΔT_g(ABS) in the ABS-rich phase is at a maximum with PC15, as shown in Table III.

Tensile and Flexural Properties

The general trends obtained (data not shown) from the tensile and flexural properties of PC/ABS blends with different component ratios are very

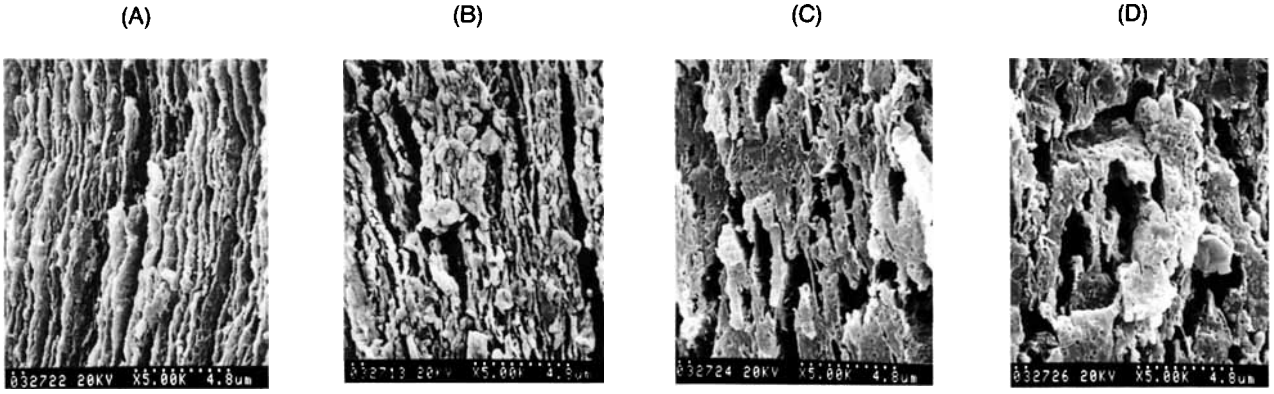

Figure 9 Etched SEM skin morphologies of PC15/ABS = 65/35 blend annealed at different times at 175°C: (A) before annealing; (B) annealed 5 min; (C) annealed 10 min; (D) annealed 15 min.

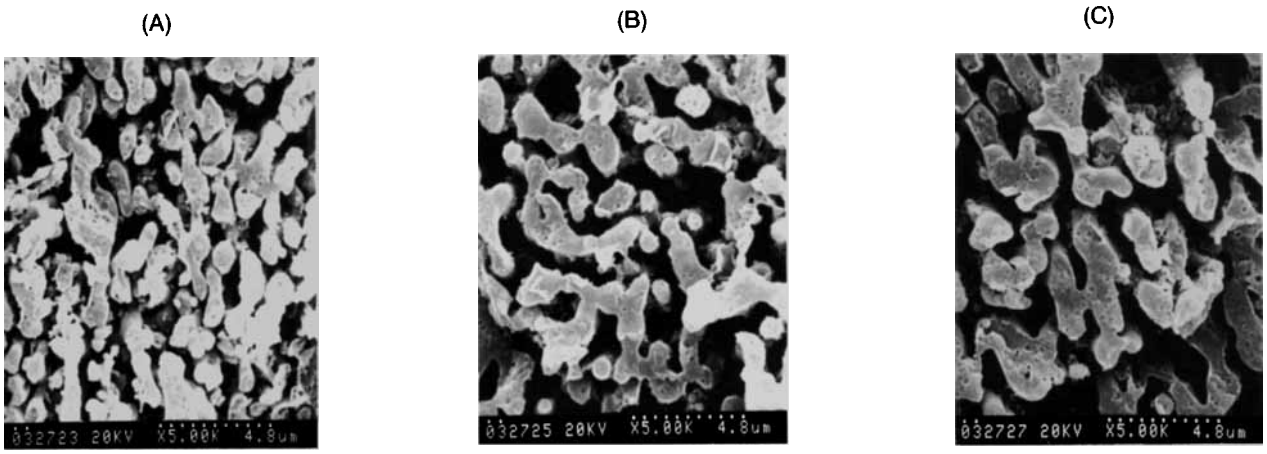

Figure 10 Etched SEM core morphologies of PC15/ABS = 65/35 blend annealed at different times at 175°C: (A) annealed 5 min; (B) annealed 10 min; (C) annealed 15 min.

similar to most literature previously reported.[14,15,20,21] Modulus and yield strength are essentially additive, but tensile elongation at break has a pronounced minimum when plotted against blend composition. Table IV shows the results of the blends with varying PC molecular weight. Modulus and yield strength are essentially identical within experimental error, whereas the blend with PC3 shows an exceptionally high tensile elongation relative to other blends.

Izod Impact Properties

Figure 11 illustrates the Izod impact strength of the PC15/ABS blends at different temperatures. The ductile–brittle transition temperature (DBTT) decreases with the increase of ABS content up to 50% of ABS. This is a typical result similar to any rubber-toughening thermoplastic system. Relative to PC, the impact strength of a PC/ABS blend is lower when the fracture is in the ductile mode but is higher in the brittle mode, similar to the rubber-toughening PCs that we reported previously.[29] When the PC content is less than 50%, the ductile–brittle transition phenomenon is not very clearly defined and the toughening efficiency is poor. Figure 12 shows similar plots for the PC/ABS blends by varying PC MFR. Higher PC molecular weight results in lower DBTT and greater fracture strength in both ductile and brittle modes. This result is not unexpected if we compare them with virgin PC with different molecular weights, as shown in Figure 13.

Table II T_g of PC15/ABS Blends with Various Component Ratios

PC/ABS	PC-rich Phase T_g (PC)	ABS-rich Phase T_g (ABS)
100/0	146.7	—
80/20	140.4	—
65/35	138.6	111.2
50/50	135.3	110.6
35/65	131.7	109.7
20/80	130.3	107.7
0/100	—	101.1

Critical Strain Energy Release Rate, *Gc*

A fracture mechanics approach to impact testing was developed independently by Brown[31] and Marshall et al.[32] by assuming the specimen to exhibit bulk linear elastic behavior. This method allows for small-scale yielding at the notch tip providing that it still possesses bulk linear elastic behavior. Sometimes, a small correction may be made to the crack length ($a + r_p$, where r_p is the plastic zone radius) to improve the accuracy of the calculation. Therefore, the experiments were purposely carried out at low temperature (−40°C) and with a sharper notch (0.125 mm notch radius) to meet the criteria of this method as closely as possible. The elastic energy, *Uc*, absorbed as strain energy by the specimen at fracture, can be expressed in terms of the compliance, *C*:

$$U_c = \tfrac{1}{2} P_c^2 C \qquad (1)$$

where P_c is the load at the onset of crack propaga-

Table III T_g (PC), T_g (ABS), ΔT_g (PC), and ΔT_g (ABS) of PC and PC/ABS = 65/35 Blends

Composition	T_g, PC	T_g, ABS	ΔT_g (PC) in PC	ΔT_g (ABS) in SAN
PC3	153.2	—	—	—
PC3/ABS	141.3	107.7	11.9	6.6
PC6	149.4	—	—	—
PC6/ABS	139.0	108.6	10.4	7.5
PC10	149.0	—	—	—
PC10/ABS	138.9	110.3	10.1	9.2
PC15	146.7	—	—	—
PC15/ABS	138.6	111.2	8.1	10.1
PC20	148.5	—	—	—
PC20/ABS	139.7	109.9	8.8	8.8
PC60	143.5	—	—	—
PC60/ABS	135.8	108.6	7.7	7.5
ABS2	—	101.1		

Table IV Tensile and Flexural Properties of PC/ABS = 65/35 Blends with Varying PC Melt Flowrate

	PC MFR					
	PC3	PC6	PC10	PC15	PC20	PC60
Tensile						
Modulus (MPa)	1880	1880	1840	1850	1870	1880
Yield stress (MPa)	62.6	60.3	59.2	63.6	61.8	62.0
Elongation (%)	88	33	31	35	35	26
Flexural						
Modulus (MPa)	2050	2190	2020	2020	2170	2120
Yield stress (MPa)	88	91	89	84	91	89

tion. The critical strain energy release rate or fracture energy, G_c, derived from linear elastic fracture mechanics, can be expressed by the following equation:

$$G_c = \frac{P_c^2}{2B} \times \frac{dC}{da} \quad (2)$$

where B is the specimen thickness and a is the crack

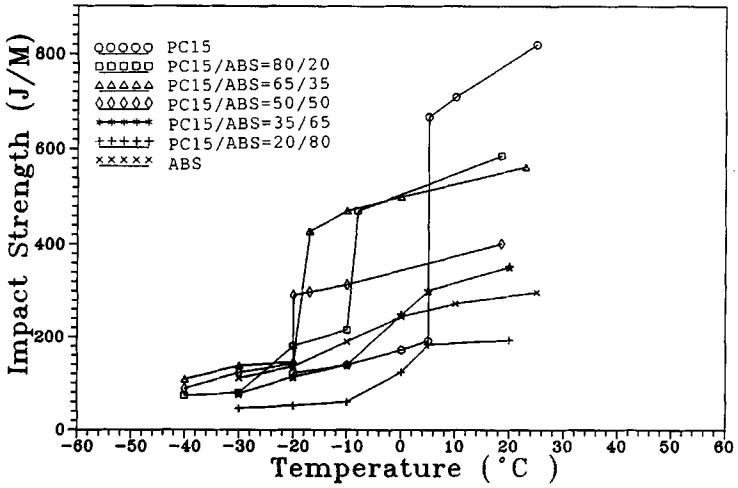

Figure 11 Izod impact strength vs. temperature of PC15/ABS blends by varying component ratios.

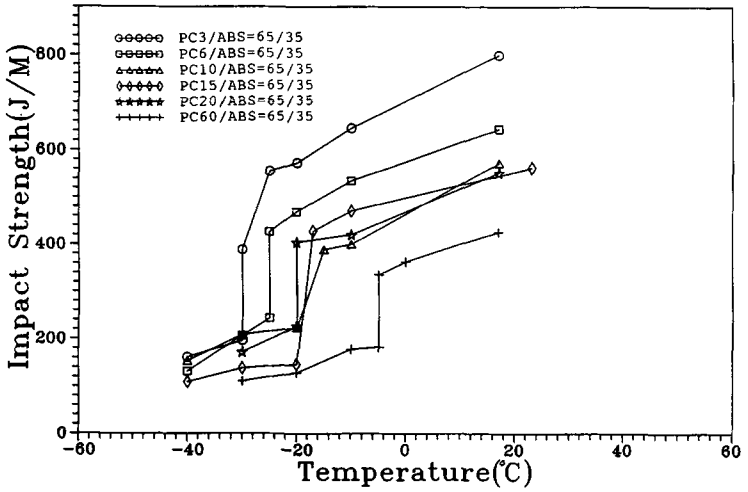

Figure 12 Izod impact strength vs. temperature of PC/ABS = 65/35 blends by varying PC MFR.

length. By substituting eq. (1) into eq. (2) and rearranging, the following equation can be obtained:

$$U_c = G_c \times B \times \frac{C}{dC/da} \tag{3}$$

Equation (3) can be expressed in the following equation by introducing the specimen width, D, and the dimensionless geometric factor, ϕ:

$$\phi = \frac{C}{dC/d(a/D)} \tag{4}$$

$$U_c = G_c \times B \times D \times \phi \tag{5}$$

Figures 14 and 15 show the plots of $B \times D \times \phi$ vs. impact energies of various PC/ABS blends. The corresponding Gc was calculated from the slope of the graph and the results are summarized in Table V. The blends with co-continuous phase structure,

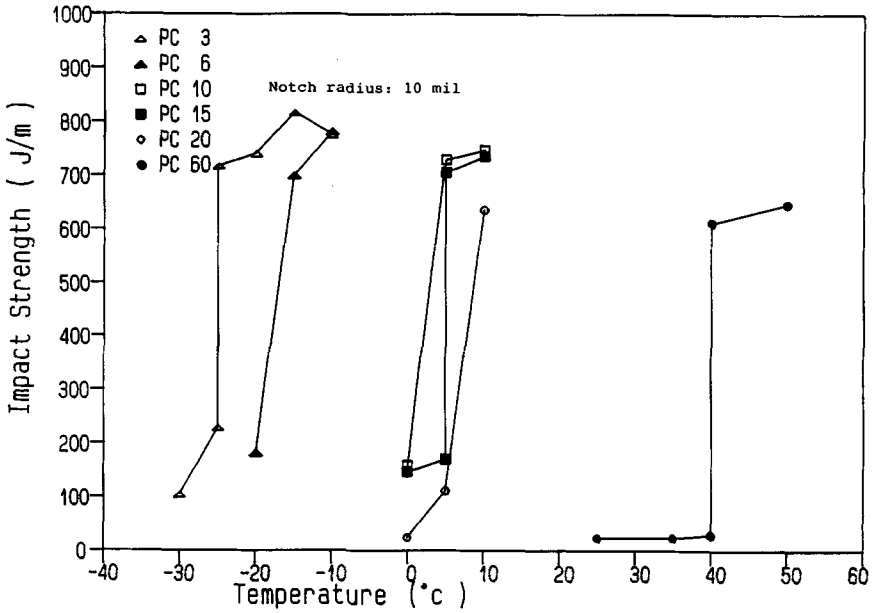

Figure 13 Izod impact strength vs. temperature of PC by varying PC MFR.

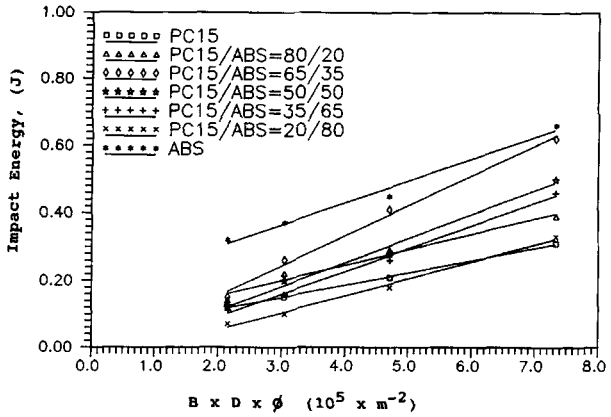

Figure 14 Plots of impact energy vs. $B \times D \times \phi$ for PC15/ABS blends with different component ratios at −40°C.

Table V Fracture Energies, *Gc*, of Various PC/ABS Blends

Composition	*Gc* (kJ/m²)
PC15	3.68
PC15/ABS = 80/20	4.59
PC15/ABS = 65/35	8.91
PC15/ABS = 50/50	7.15
PC15/ABS = 35/65	6.78
PC15/ABS = 20/80	5.09
ABS	6.53
PC3/ABS = 65/35	13.30
PC6/ABS = 65/35	9.86
PC10/ABS = 65/35	8.75
PC20/ABS = 65/35	8.03
PC60/ABS = 65/35	5.32

65 and 50% in PC15, show higher *Gc* values and this range of the component ratio is of commercial interest. For the blend with varying PC molecular weight and at a fixed component ratio, PC/ABS = 65/35, the resulting *Gc* increases with the increase of PC molecular weight. The blend with the lowest molecular weight PC60 has the lowest *Gc* value. Fracture toughness of PC is highly sensitive to its molecular weight, relative to other polymers, even above its critical entanglement molecular weight as reported previously.[29] These observed results are not unexpected since the PC is the major component in the PC/ABS = 65/35 blends.

CONCLUSIONS

1. Melt viscosities of PC/ABS blends relative to pure PC are significantly lower, even lower than those of pure ABS in several compositions.
2. The observed ΔT_g(PC) in the PC-rich phase and ΔT_g(ABS) in the ABS-rich phase are comparable, an indication of close mutual solubility of the two phases.
3. Annealing above T_g of PC coarsens the phase structure of the blend.
4. Higher PC molecular weight has the tendency to raise the viscosity of the PC/ABS blend.
5. Higher PC molecular weight increases the ductility of the blends in terms of lower DBTT and higher impact strength.
6. The critical strain energy release rate, *Gc*, of the blend has a similar trend as that of the observed impact strength.
7. The component ratio of PC/ABS = 65/35 can be considered as a compromise composition in terms of the product toughness, cost, and the processing melt viscosity.
8. The toughness advantages by increasing PC molecular weight must be compensated by the viscosity increase and this fact has to be taken into consideration in selecting the starting materials.

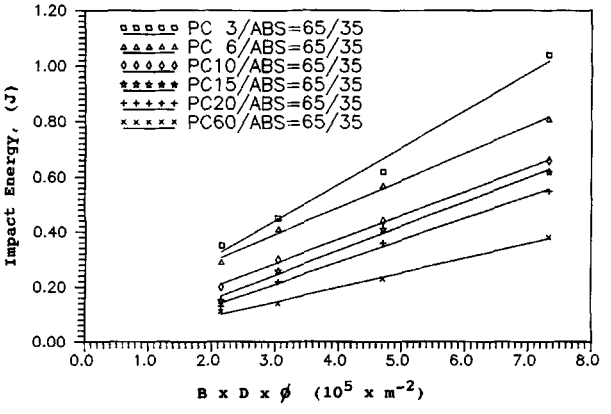

Figure 15 Plots of impact energy vs. $B \times D \times \phi$ for PC/ABS = 65/35 blends by varying PC MFR at −40°C.

REFERENCES

1. T. S. Grabowski, U.S. Pat. 3,130,177 (1964) (to Borg-Warner Corp.).
2. S. Furukawa et al., Jpn. Kokai 73,43,750 (1973) (to Daicell Co. Ltd.).
3. R. Hasegawa et al., Jpn. Kokai 74,04,745 (1974) (to Teijin Ltd.).

4. E. Yonemitsu et al., Jpn. Kokai 75,85,651 (1975) (to Mitsubishi Gas Chemical Co.).
5. T. Kotani et al., Jpn. Kokai 76,128,356 (1976) (to Japan Synthetic Rubber Co.).
6. D. E. Henton, U.S. Pat. 4,218,544 (1980) (to Dow Chemical Co.).
7. D. Margotte et al., Ger. Offen. 3,002,662 (1981) (to Bayer A.G.).
8. P. Y. Liu, U.S. Pat. 4,390,657 (1983) (to General Electric).
9. U. R. Grigo et al., U.S. Pat. 4,472,554 (1984) (to Mobay Chemical Co.).
10. K. C. Rusch and R. H. Beck, *J. Polym. Sci. Part C,* **30,** 447 (1970).
11. D. Stefan and H. L. Williams, *J. Appl. Polym. Sci.,* **18,** 1451 (1974).
12. V. Dobrescu and V. Cobxaru, *J. Polym. Sci. Polym. Symp.,* **64,** 27 (1978).
13. S. L. Cohen and N. R. Lazear, *Plast. Eng.,* **Aug.,** 23 (1982).
14. T. Kusauchi and T. Ohta, *J. Mater. Sci.,* **19,** 1699 (1984).
15. H. Suarez, J. W. Barlow, and D. R. Paul, *J. Appl. Polym. Sci.,* **29,** 3253 (1984).
16. D. Keitz, J. W. Barlow, and D. R. Paul, *J. Appl. Polym. Sci.,* **29,** 3131 (1984).
17. K. Koo, T. Inoue, and K. Miyasaka, *Polym. Eng. Sci.,* **25,** 741 (1985).
18. G. Weber and J. Schocps, *Angew. Makromol. Chem.,* **136,** 45 (1985).
19. R. E. Skochdopolc, C. R. Finch, and J. Marshall, *Polym. Eng. Sci.,* **27,** 627 (1987).
20. W. Y. Chiang and D. S. Hwung, *Polym. Eng. Sci.,* **27,** 632 (1987).
21. W. K. Chin and J. L. Hwang, in *Advances in Polymer Blends and Alloys Technology,* M. A. Kohudic, Ed., Technomic, Lancaster, 1988, Vol. 1, p. 154.
22. W. N. Kim and C. M. Burns, *Polym. Eng. Sci.,* **28,** 1115 (1988).
23. K. W. Mclaughlin, *Polym. Eng. Sci.,* **29,** 1560 (1989).
24. D. Quintens, G. Groeninckx, M. Guest, and L. Aerts, *Polym. Eng. Sci.,* **30,** 1474, 1484 (1990).
25. J. J. Herpels and L. Mascia, *Eur. Polym. J.,* **26,** 997 (1990).
26. M. Ishikawa and I. Chiba, *Polymer,* **31,** 1232 (1990).
27. F. C. Chang and M. Y. Yang, *Polym. Eng. Sci.,* **30,** 543 (1990).
28. F. C. Chang and Y. C. Hwu, *Polym. Eng. Sci.,* **31,** 1509 (1991).
29. F. C. Chang, J. S. Wu, and L. H. Chu, *J. Appl. Polym. Sci.,* **44,** 491 (1992).
30. F. C. Chang and H. C. Hsu, *J. Appl. Polym. Sci.,* **43,** 1025 (1991).
31. H. R. Brown, *J. Mater. Sci.,* **8,** 941 (1973).
32. G. P. Marshall, J. G. Williams, and E. E. Turner, *J. Mater. Sci.,* **8,** 949 (1973).

Received August 24, 1992
Accepted March 3, 1993